Succinate Secreted by Trypanosoma brucei Is Produced by a Novel and Unique Glycosomal Enzyme, NADH-dependent Fumarate Reductase

Sébastien Besteiro, Marc Biran, Nicolas Biteau, Virginie Coustou, Theo Baltz, Paul Canioni, Frédéric Bringaud

▶ **To cite this version:**

Sébastien Besteiro, Marc Biran, Nicolas Biteau, Virginie Coustou, Theo Baltz, et al.. Succinate Secreted by Trypanosoma brucei Is Produced by a Novel and Unique Glycosomal Enzyme, NADH-dependent Fumarate Reductase. Journal of Biological Chemistry, 2002, 277 (41), pp.38001-38012. 10.1074/jbc.M201759200 . hal-02378776

HAL Id: hal-02378776
https://hal.science/hal-02378776v1

Submitted on 27 May 2021

HAL is a multi-disciplinary open access archive for the deposit and dissemination of scientific research documents, whether they are published or not. The documents may come from teaching and research institutions in France or abroad, or from public or private research centers.

L'archive ouverte pluridisciplinaire **HAL**, est destinée au dépôt et à la diffusion de documents scientifiques de niveau recherche, publiés ou non, émanant des établissements d'enseignement et de recherche français ou étrangers, des laboratoires publics ou privés.

Distributed under a Creative Commons Attribution 4.0 International License

THE JOURNAL OF BIOLOGICAL CHEMISTRY
Vol. 277, No. 41, Issue of October 11, pp. 38001–38012, 2002
Printed in U.S.A.
© 2002 by The American Society for Biochemistry and Molecular Biology, Inc.

Succinate Secreted by *Trypanosoma brucei* Is Produced by a Novel and Unique Glycosomal Enzyme, NADH-dependent Fumarate Reductase

Received for publication, February 21, 2002, and in revised form, June 25, 2002
Published, JBC Papers in Press, July 22, 2002, DOI 10.1074/jbc.M201759200

Sébastien Besteiro‡, Marc Biran§, Nicolas Biteau‡, Virginie Coustou‡, Théo Baltz‡, Paul Canioni§, and Frédéric Bringaud‡¶

From the ‡Laboratoire de Parasitologie Moléculaire, UMR-5016 CNRS and §Résonance Magnétique des Systèmes Biologiques, UMR-5536 CNRS, Université Victor Segalen Bordeaux II, 146 Rue Léo Saignat, 33076 Bordeaux Cedex, France

In all trypanosomatids, including *Trypanosoma brucei*, glycolysis takes place in peroxisome-like organelles called glycosomes. These are closed compartments wherein the energy and redox (NAD^+/NADH) balances need to be maintained. We have characterized a *T. brucei* gene called *FRDg* encoding a protein 35% identical to *Saccharomyces cerevisiae* fumarate reductases. Microsequencing of FRDg purified from glycosome preparations, immunofluorescence, and Western blot analyses clearly identified this enzyme as a glycosomal protein that is only expressed in the procyclic form of *T. brucei* but is present in all the other trypanosomatids studied, *i.e. Trypanosoma congolense*, *Crithidia fasciculata* and *Leishmania amazonensis*. The specific inactivation of *FRDg* gene expression by RNA interference showed that FRDg is responsible for the NADH-dependent fumarate reductase activity detected in glycosomal fractions and that at least 60% of the succinate secreted by the *T. brucei* procyclic form (in the presence of D-glucose as the sole carbon source) is produced in the glycosome by FRDg. We conclude that FRDg plays a key role in the energy metabolism by participating in the maintenance of the glycosomal NAD^+/NADH balance. We have also detected a significant pyruvate kinase activity in the cytosol of the *T. brucei* procyclic cells that was not observed previously. Consequently, we propose a revised model of glucose metabolism in procyclic trypanosomes that may also be valid for all other trypanosomatids except the *T. brucei* bloodstream form. Interestingly, H. Gest has hypothesized previously (Gest, H. (1980) *FEMS Microbiol. Lett.* 7, 73–77) that a soluble NADH-dependent fumarate reductase has been present in primitive organisms and evolved into the present day fumarate reductases, which are quinol-dependent. FRDg may have the characteristics of such an ancestral enzyme and is the only NADH-dependent fumarate reductase characterized to date.

Fumarate reductase (FRD)[1] catalyzes the reduction of fumarate to succinate, using as an electron donor a quinol such as menaquinol (1) or $FADH_2$/$FMNH_2$ (2). This enzyme plays a key role in the anaerobic metabolism of many prokaryotes and eukaryotes (green algae, parasitic helminths, yeast, and some lower marine organisms) (1, 3). Most of the FRDs characterized to date are membrane-bound proteins closely related to the tricarboxylic acid cycle enzyme succinate dehydrogenase, which catalyzes the reverse reaction (the oxidation of succinate) (1). These FRD enzymes belong to a multimeric complex embedded in the mitochondrial membrane that is similar to complex II of the respiratory chain (succinate dehydrogenase complex), which is part of an electron transfer chain. In this case, FRD transfers electrons from a quinol to a fumarate, which is the terminal electron acceptor and thus is directly involved, under anaerobic conditions, in ATP production by oxidative phosphorylation. In contrast, the FRDs described in *Shewanella putrefaciens* (4) and *Saccharomyces cerevisiae* (2) are soluble proteins not associated with membrane-bound multimeric complexes. Although soluble, the *Shewanella* FRD seems to be involved in an electron transfer chain with a quinol as the electron donor as observed for the membrane-bound FRD (4). However, the yeast FRD is unique, because this soluble enzyme uses $FADH_2$/$FMNH_2$ as electron donor, is not linked to an electron transfer chain, and is not involved in oxidative phosphorylation (2, 5).

The trypanosomatid family is composed of protists belonging to the order Kinetoplastida, which represents one of the earliest evolutionary branches in the eukaryotic lineage. All known trypanosomatids are parasites, and some of them cause serious diseases in man (*Leishmania*, *Trypanosoma cruzi*, and the African trypanosomes *Trypanosoma brucei gambiense* and *Trypanosoma brucei rhodesiense*), domestic animals (many African trypanosome species), and plants (*Phytomonas*). During their life cycle, African trypanosomes (including *T. brucei*) differentiate into several adaptive forms, the most prominent being the bloodstream form in the mammalian host and the procyclic form in the midgut of the tsetse fly vector. In all trypanosomatids most glycolytic enzymes are found in specific organelles, the glycosomes, which are microbody-like organelles related to peroxisomes (6, 7).

The bloodstream form of the *T. brucei* group possesses a

* This work was supported by the CNRS, grants from the Conseil Régional d'Aquitaine, the GDR-CNRS, the French Ministère de l'Education Nationale de la Recherche et de la Technologie (Action Microbiologie), and European Commission INCO-Dev Program Grant ICA4-CT-2001-10075). The costs of publication of this article were defrayed in part by the payment of page charges. This article must therefore be hereby marked "*advertisement*" in accordance with 18 U.S.C. Section 1734 solely to indicate this fact.

The nucleotide sequence(s) reported in this paper has been submitted to the GenBank™/EBI Data Bank with accession number(s) AF457132.

¶ To whom correspondence should be addressed. Tel.: 33-5-5757-4632; Fax: 33-5-5757-1015; E-mail: bringaud@u-bordeaux2.fr.

[1] The abbreviations used are: FRD, fumarate reductase; RNAi, RNA interference; TIGR, The Institute for Genomic Research; PBS, phosphate-buffered saline; PPDK, pyrovate phosphate dikinase; GPDH, glycerol-3-phosphate dehydrogenase; PEP, phosphoenolpyruvate; PEPCK, PEP carboxykinase; PYK, pyruvate kinase; PGK, phosphoglycerate kinase; CoA, coenzyme A.

This is an Open Access article under the CC BY license.

unique and simple energy metabolism as compared with all other adaptative forms of trypanosomatids (8, 9). The *T. brucei* bloodstream form converts D-glucose into 3-phosphoglycerate inside the glycosome, whereas the last three steps leading to pyruvate are in the cytosol (7). The absence of a tricarboxylic acid cycle and a respiratory system coupled to ATP synthesis implies that all of the ATP required for anabolic pathways is produced by the cytosolic pyruvate kinase with the pyruvate being the only end product secreted under aerobic conditions.

In contrast, all other trypanosomatid adaptative forms, including the procyclic form of the *T. brucei* group, have a mitochondrion functional in ATP production coupled to aerobic respiration (6, 10). In addition, these parasites may produce several incompletely oxidized products of aerobic fermentation such as ethanol, succinate, acetate, alanine, pyruvate, and glycerol and/or lactate (10). All of these parasites secrete succinate, but the pathway(s) leading to succinate production is (are) not clearly understood (8, 10). Succinate may be produced by the conventional tricarboxylic acid cycle as proposed previously (6, 8) or by a soluble NADH-dependent FRD activity, which has been described in the *T. brucei* procyclic form (11), the *T. cruzi* epimastigote form (12), and the *Leishmania* sp. promastigote form (13). However, the nature of the enzyme(s) responsible for the production of the secreted succinate is still debated as is the relevance of this activity in the energy metabolism of the trypanosomatid and its subcellular localization (8, 14, 15).

Recently, Ngô *et al.* (16) showed that the transfection of *T. brucei* with double-stranded RNA results in specific degradation of the targeted gene transcript (17) by RNA interference (RNAi). This approach was adapted to constitutive or inducible expression in *T. brucei* and proved to be extremely powerful in determining the function of gene products (18–22). The RNAi tool has not yet been adapted to the other human pathogens, *i.e. Leishmania* sp. and *T. cruzi*. However, when studying pathways shared by all trypanosomatids such as carbohydrate metabolism, the *T. brucei* procyclic form constitutes an excellent model, and conclusions drawn from RNAi experiments with these cells may also be applicable to the other parasites.

Here, we report the identification and characterization, in the *T. brucei* procyclic form, of a novel, abundant glycosomal enzyme (FRDg) that contains an NADH-dependent FRD activity. This protein is expressed in all trypanosomatids analyzed except the bloodstream form of *T. brucei.* Specific inhibition of its expression using RNAi showed that FRDg produces at least 60% of the succinate secreted by the procyclic form of *T. brucei*. In addition, we also showed the presence of a significant pyruvate kinase activity in the cytosol of the procyclic form. Thus, on the basis of these new data we propose a revision in the current model of glycosomal and mitochondrial carbohydrate metabolism in trypanosomatids that was established about 15 years ago (6, 10).

EXPERIMENTAL PROCEDURES

Trypanosome and Glycosome Preparations—The bloodstream form of *T. brucei* AnTat1 was grown in rats and isolated by DEAE ion exchange chromatography as described previously (23). The procyclic form of *T. brucei* EATRO1125 was cultured at 27 °C in SDM-79 medium containing 10% (v/v) fetal calf serum and 3.5 mg·ml^{-1} hemin (24). The AnTat1 and EATRO1125 clones were derived from the same EATRO1125/LUMP581 stabilate, isolated from a bushbuck at Mavubwe, Busoga District, Uganda in 1966 (25). The procyclic form of *Trypanosoma congolense* IL3000 clone 49 (provided by E. Authié) was grown as described previously (26). The epimastigote form of *T. cruzi* C. L. (provided by P. Minoprio, Pasteur Institute, Paris) was cultured and prepared as described (27), the *Crithidia fasciculata* clone HS6 was grown as described (28), and the promastigote form of *Leishmania amazonensis* MHOM/BR/87/BA125 was cultured at 26 °C in Iscove's medium supplemented with 10% fetal calf serum. Glycosomes were purified from procyclic (EATRO1125) and bloodstream (AnTat1) forms of *T. brucei* as described (29) after homogenizing the cells in STE buffer (250 mM sucrose, 25 mM Tris, pH 7.4, 1 mM EDTA) with silicon carbide as grinding material (30).

Peptide Sequencing of p120 and Cloning of the p120 Gene—Glycosomal proteins (500 μg) isolated from the EATRO1125 procyclic cells were separated by SDS-PAGE, blotted on nylon PSQ filters (Immobilon), and stained with Amido Schwarz. The band containing the 120-kDa protein (p120) was cut out and submitted to trypsin digestion at 25 °C for 18 h in the presence of 50 mM Tris-HCl, pH 8.6, 0.01% Tween, and 0.3 μg of trypsin. Peptides were separated by high pressure liquid chromatography, and the N-terminal extremity of major peaks as well as the undigested p120 were microsequenced as described (31). Peptide sequences and their positions on the *p120* gene product are as follows: N-term, ^{2}VDGRSSASIVAVDPERAARERDAAA^{26}; p48b, ^{152}NACLEALTQA^{161}; p40, ^{195}YIVDYVIDNINAAGFQNVF^{213}; p48a, ^{251}EASYISVISLDNEALATSGD^{270}; p39, ^{473}ADAIGWLTSLGVPLTVLSQ^{491}; p34, ^{600}EHAPHLVNFP^{609}; p25, ^{717}KLFGVSSHEFYWK^{729}; p43, ^{822}APLSHSNPILGLFGAGEVT^{840}; p32, ^{883}VWTTVVLR^{890}; and p35, ^{964}EWISALEPGDAVEMK^{978}. BLAST searches in the data base of The Institute for Genomic Research (TIGR; http://www.tigr.org/tdb/mdb/tbdb/index.html) revealed that peptides p40, p48a, and p48b are encoded by the extremities of clone SH-37B24. A PCR product (pr37B24) obtained from genomic DNA of *T. brucei* EATRO1125 by using primers derived from the SH-37B24-R sequence (TIGR data base) was used as a α-^{32}P-labeled probe to screen a genomic library of *T. brucei* AnTat1 constructed in the c2X75 cosmid vector (32). The selected CosFRD11 clone was *Hpa*I-digested and subcloned into the *Hin*cII-digested pUC18 vector (Appligene), and the resulting recombinant colonies were screened with the α-^{32}P-labeled pr37B24 probe to isolate the full-length *p120* gene, which was sequenced by the dideoxynucleotide chain termination method using AmpliTaq DNA polymerase as described by the manufacturer (ABI PRISM^{TM}, PerkinElmer Life Sciences).

Alignments and Phylogenetic Analyses—DNA and amino acid sequences were analyzed using the DNA STRIDER program, and data base searches were done with BLAST. For the phylogenetic analysis, the central domain of FRDg (from amino acid positions 406 to 839) was aligned with the corresponding region of homologous proteins (fumarate reductases and succinate dehydrogenases) from other organisms. Multiple alignment of amino acid sequences and hamming distances were obtained using Clustal W version 1.6 (33), and the phylogenetic tree was constructed using version 3.5c of the PHYLIP program package of J. Felsenstein (BLAST, Clustal W and PHYLIP were obtained through the Bisance and Infobiogen facilities). The matrix of pairwise sequence distances were calculated by Dayhoff's method using PRODIST. The unrooted phylogenetic trees were constructed from the distance matrix using the neighbor or Fitch methods. The phylogenetic tree was drawn with TREEVIEW version 1.3 (34). The statistical robustness of the resulting phylogenetic tree was assessed with the SeqBoot program by bootstrap resampling analysis generating 100 reiterated data sets. The resulting bootstrap values were added manually at each corresponding node.

Expression of an Anti-FRDg Double-stranded RNA—To inhibit FRDg expression by RNAi (16), we generated a "sense/antisense" cassette in the pLew79 expression vector (kindly provided by E. Wirtz and G. Cross) (35) that targets the 3′-end of the *FRDg* gene (195 bp) followed by 258 bp of the untranslated region. The plasmid construction was performed as reported previously for the inhibition of a flagellar protein (FTZC) expression by RNAi (19). Briefly, a PCR-amplified, 489-bp antisense sequence (453 bp of the targeted sequence plus 36 bp used as a spacer between the sense and antisense sequences) was inserted in the *Hin*dIII and *Bam*HI restriction sites of the pLew79 plasmid. Then, a PCR-amplified 453-bp sense sequence was inserted upstream of the antisense sequence in the *Hin*dIII and *Avr*II restriction sites (*Avr*II was introduced at the 5′ extremity of the antisense PCR fragment). The resulting plasmid, pLew-FRDg-SAS, contained a chimeric construct composed of the sense and antisense version of a *FRDg* gene fragment, separated by a 36-bp fragment, under the control of the tetracycline-inducible poly(ADP-ribose) polymerase promoter (35). The EATRO1125 procyclic form cell line (EATRO1125.T7T) expressing the T7 RNA polymerase gene and the tetracycline repressor under the dependence of a T7 RNA polymerase promoter for inducible control by tetracycline (19) or wild type EATRO1125 procyclic cells were transformed with the pLew-FRDg-SAS plasmid. Trypanosome transfection and selection of phleomycin-resistant clones were performed as reported previously (19, 36).

Enzymatic Activities—Sonicated (5 s at 4 °C) crude extracts of trypanosomes resuspended in STE buffer and glycosomal fractions resuspended in STE buffer were tested for enzymatic activities. For

NADH-dependent fumarate reductase and cytochrome *c* reductase assays, succinate or reduced cytochrome *c* formation was measured spectrophotometrically at 340 nm via oxidation of NADH (11). Pyruvate kinase activity was measured in the absence of its activator (fructose 2,6-bisphosphate) as described (37). Glycerol-3-phosphate dehydrogenase (38), phosphoglycerate kinase (PGK) (39), phosphoenolpyruvate carboxykinase (40), isocitrate dehydrogenase (41), citrate synthase (42), and fumarase (43) activities were all measured according to published procedures.

D-Glucose and pH Measurements in Growth Medium—To determine the rate of D-glucose consumption, 10^9 procyclic cells (exponential phase) were collected by centrifugation, washed in PBS buffer, and resuspended in 10 ml of fresh SDM-79 medium containing 10% calf serum. The cells were incubated for 8 h, and samples (50 μl) were collected at 30 min intervals. Each sample was centrifuged at 14,000 $\times$ *g* for 30 s, and the quantity of D-glucose remaining in the supernatant was determined using a glucose trinder kit (Sigma). For pH measurements, procyclic cells (10^5 cells·ml^{-1}) were grown in 20 ml of SDM-79 medium containing 10% calf serum until reaching the stationary phase (after about 5 days). The pH value was determined on the supernatant of centrifuged aliquots (1 ml) using a pH meter.

Digitonin Permeabilization—Procyclic EATRO1125 cells were washed in PBS buffer and resuspended at 6.5×10^8 cells·ml^{-1} (3.3 mg of protein) in STE buffer supplemented with 150 mM NaCl and the Complete™ mini EDTA-free protease inhibitor mixture (Roche Molecular Biochemicals). Cell aliquots (300 μl) were incubated for 4 min at 25 °C with increasing concentrations of digitonin before being centrifuged at 14,000 $\times$ *g* for 2 min as described previously (44). Enzymatic activities that were released from the cells were assayed in the supernatants.

Production of FRDg Antibodies and Detection of FRDg—A synthetic peptide corresponding to the 23 C-terminal amino acids of the p120 protein and containing an additional N-terminal cysteine residue (CTLGYNMNLVRTVDETEPSGSSKI) was covalently linked to an ovalbumin carrier and used to immunize a rabbit as described (45). The p120 specific antibodies were purified by affinity chromatography using the same peptide covalently linked to activated CH-Sepharose 4B resin (Amersham Biosciences) as described by the manufacturer.

For Western blot analyses, total extracts of the bloodstream form AnTat1 and procyclic form EATRO1125 of *T. brucei* (10^7 cells) or glycosomal fractions of the same parasites (10 μg of protein) were separated by SDS-PAGE (8%) and immunoblotted on Immobilon-P filters (Millipore) (45). Immunodetection was performed as described (45, 46) using, as primary antibodies, affinity-purified anti-FRDg and rabbit anti-GPDH (36, 38) diluted 1:100 and, as secondary antibodies, anti-mouse and anti-rabbit IgG conjugated to horseradish peroxidase (Bio-Rad), respectively.

For immunofluorescence analyses, log phase cells were fixed with formaldehyde as described previously (36). Slides were incubated with affinity-purified anti-FRDg antibodies and monoclonal mouse anti-PPDK H112 followed by fluorescein isothiocyanate-conjugated goat anti-rabbit secondary antibody diluted 1:100 (Bio-Rad) and Alexa Fluor 568-conjugated goat anti-mouse secondary antibody diluted 1:100 (Molecular Probes), respectively. Cells were viewed with a Zeiss UV microscope, and images were captured by a MicroMax-1300Y/HS camera (Princeton Instruments) and MetaView software (Universal Imaging) and merged in Adobe Photoshop on a Macintosh iMac computer.

Nuclear Magnetic Resonance Experiments—4×10^9 *T. brucei* procyclic cells were collected by centrifugation at 1,400 $\times$ *g* for 10 min, washed once in PBS buffer, and incubated in 10 ml of incubation buffer (PBS buffer supplemented with 24 mM $NaHCO_3$, pH 7.3) containing 11 mM D-[1-^{13}C]glucose (110 μmole) for 90–180 min at 27 °C. D-glucose concentration in the medium was determined with the D-glucose trinder kit (Sigma). The integrity of the cells during the incubation was checked by microscopic observation. After centrifugation for 10 min at 1,400 $\times$ *g*, the supernatant was lyophilized, resuspended in 500 μl of D_2O, and 50 μl of pure dioxane was added as an external reference. ^{13}C NMR spectra were collected at 100.6 MHz. Measurements were recorded at 25 °C with a proton composite pulse decoupling. Acquisition conditions were 90° flip angle, 22.15 kHz spectral width, 64K memory size, and 21.5-s total recycle time. Measurements were performed overnight with 2,048 scans. Spectra were collected after a 1 Hz exponential line broadening. ^{1}H-NMR spectra were recorded at 400 MHz and referenced to the dioxane resonance at 3.75 ppm. The residual water signal was reduced by homonuclear presaturation. Spectra were collected using 90° flip angle, 6-s relaxation delay, 8.05-s total recycle time, 4-KHz spectra width, and 32K memory size. The specific ^{13}C enrichment of lactate (C3), acetate (C2), fumarate, L-malate, and succinate (C2 and C3) were determined from ^{1}H-NMR spectra as the ratio of the area of the satellites (^{13}C-^{1}H coupling) to the total area of the corresponding multiplet. The amount of secreted products was calculated on the basis of the specific enrichment values and the carbon-13 content for each metabolite at the position of interest using the enriched C1 glucose as a quantitative reference.

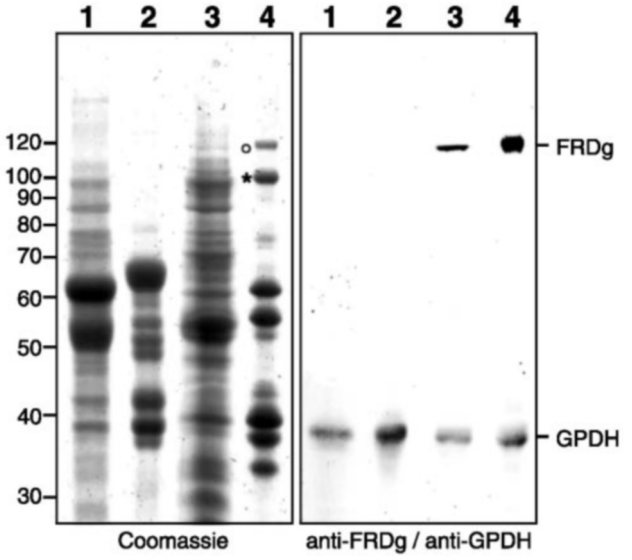

FIG. 1. **The expression pattern of FRDg in *T. brucei* by Western blot analysis.** Lysates of 2×10^7 cells (*lanes 1* and *3*) or 20 μg of glycosomal proteins (*lanes 2* and *4*) from the AnTat1 bloodstream form (*lanes 1* and *2*) or the EATRO1125 procyclic form (*lanes 3* and *4*) were analyzed by Coomassie staining (*left panel*) or with anti-FRDg serum and then reprobed with anti-GPDH immune serum (*right panel*). The positions of FRDg and GPDH are indicated in the *right margin*, and the molecular mass markers (in kDa) are indicated in the left margin. The *open circle* and *asterisk* in *lane 4* of the Coomassie-stained panel indicate FRDg and PPDK, respectively.

RESULTS

Cloning of a Trypanosoma brucei Gene Encoding a Glycosomal Putative Multifunctional Protein—We previously characterized a pyruvate phosphate dikinase (PPDK) as a 97-kDa glycosomal protein expressed in the procyclic form but absent in the bloodstream form of *T. brucei* (36). In the course of this study, an abundant 120-kDa glycosomal protein (p120) presenting the same differential expression was detected (Fig. 1*A*). To characterize this unknown protein, it was purified from glycosomal fractions, and nine peptides generated by its tryptic digestion were purified and microsequenced. In addition, the N-terminal extremity of the purified p120 protein was sequenced. A DNA fragment (SH-37B24-R) encoding 3 of 10 p120 peptidic sequences was identified in the *T. brucei* GSS data base (www.tigr.org/tdb/mdb/tbdb/index.html) and used as a probe to clone (from a *T. brucei* cosmid genomic library) a full-length gene encoding a 1142-amino acid protein that contains all 10 peptidic sequences generated from the isolated p120 glycosomal protein. The position of each peptidic sequence is positioned on the p120 map shown in Fig. 2*A*. In addition, the encoded protein is basic (calculated isoelectric point 9.64) as are many other glycosomal proteins of *T. brucei* (47), and the last three amino acids (SKI) correspond to a type 1 peroxisome-targeting signal (48), providing further evidence that this gene encodes the glycosomal 120-kDa protein.

By BLAST analysis, the best score was obtained with the fumarate reductase (EC 1.3.1.6) from *S. cerevisiae*, which shares 35% identity with the central region (corresponding to the amino acids from position 406 to 839). Thus, the p120 protein was called FRDg for glycosomal fumarate reductase. Considering the probable involvement of FRDg in succinate production by the *T. brucei* procyclic form and the other human

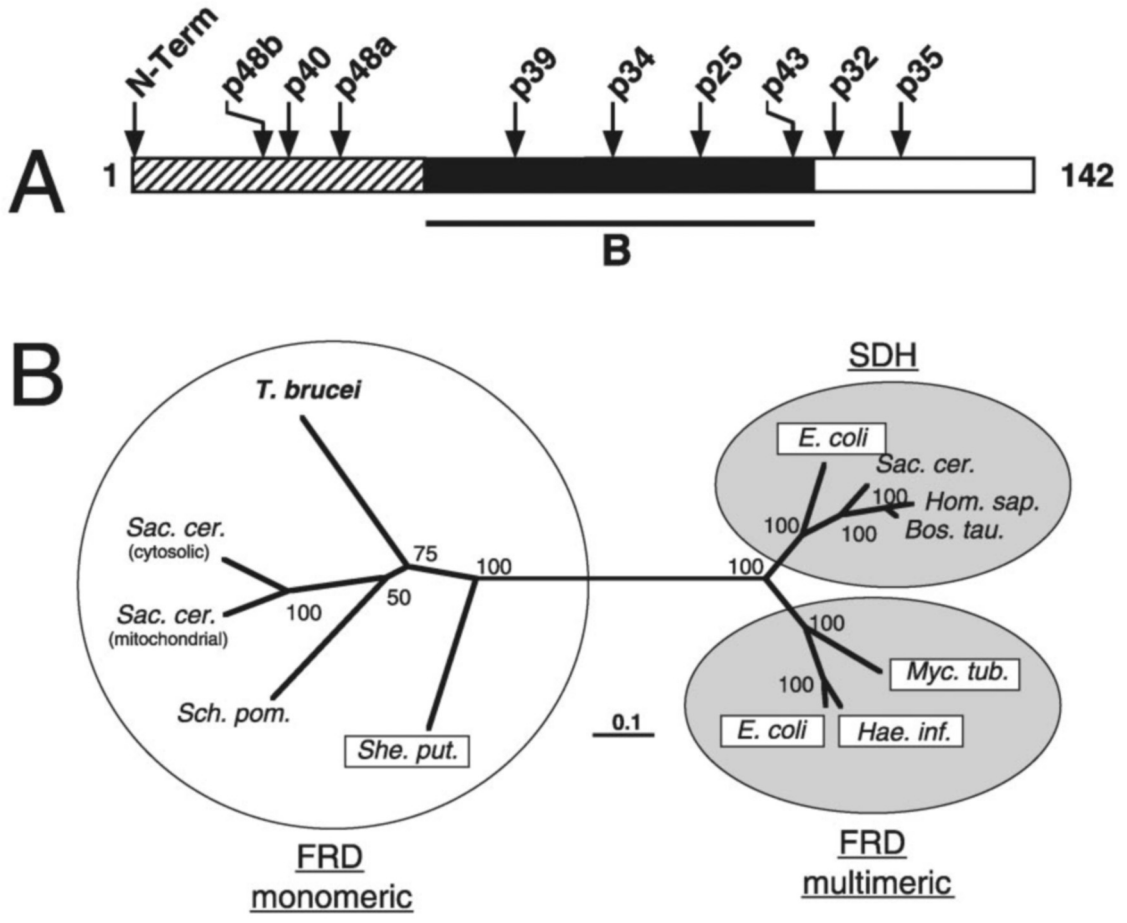

FIG. 2. **Comparison of the central domain constituting the p120 proteins with homologous proteins from other organisms.** *A*, the domains homologous to proteins involved in thiamine synthesis (*shaded box*), NADH-dependent fumarate reductases (*black box*), and cytochrome b_5 reductases/nitrate reductases (*white box*) are located on the schematic representation of the p120 protein. The position and name of all the peptides sequenced from the isolated p120 and the region used for the phylogenetic analysis (*area B*) are indicated above and under the map, respectively. *B*, the phylogenetic tree was constructed from the alignment of the B region of p120 with monomeric and multimeric FRD and succinate dehydrogenases. The unrooted tree was obtained by distance-based analyses (neighbor joining and Fitch-Margoliash methods) using the complete amino acid sequence deleted from the N- and C-terminal non-homologous regions. The *scale bar* represents a genetic distance of 0.1 amino acid substitution per site, and the numbers given on each node represent the percentage of bootstrap replicas yielding this tree. Sequences from prokaryotes are boxed and grouped according to their function. Abbreviations and/or Swiss-Prot accession numbers are: *Bos. tau*., *Bos taurus* (P31039); *E. coli*, (P00363 and X00980); *Hae. inf*., *Haemophilus influenzae* (P44894); *Hom. sap*., *Homo sapiens* (P31040); *Myc. tub*., *Mycobacterium tuberculosis* (Z74020); *Sac. cer*., *Saccharomyces cerevisiae* (P21375, M86746, and P32614); *Sch. pom*., *Schizosaccharomyces pombe* (Z99292); *She. put*., *Shewanella putrefaciens* (Q02469).

pathogenic trypanosomatids, we aimed to determine its role in the carbohydrate metabolism of these parasites.

FRDg Is a Potentially Multifunctional Protein—Three domains (N-terminal, central, and C-terminal) can be distinguished in FRDg (Fig. 2*A*), each having homologues in the Swiss-Prot data base. As mentioned above, the central domain is homologous to fumarate reductases. When FRDg was included in a phylogenetic analysis of well characterized FRD proteins, it appeared to be closely related to all the soluble/monomeric FRDs (yeasts and *Shewanella putrefasciens*), which form a monophyletic group distant from multimeric FRD and succinate dehydrogenases (Fig. 2*B*). The best score obtained by BLAST analysis for the N-terminal domain (from position 37 to 324) is with the ApbE protein (involved in thiamine biosynthesis) (49) from *Neisseria meningitidis* (27% identity). Interestingly, FRDg is the only eukaryotic protein characterized to date that is homologous to these prokaryotic proteins. The C-terminal domain (from position 906 to 1128) is related to cytochrome b_5 reductases and the cytochrome domain of nitrate reductases, which belong to the flavoprotein pyridine nucleotide cytochrome reductase family (50). This FRDg domain is 29 and 27% identical to the cytochrome b_5 reductase and the cytochrome domain of nitrate reductase from *Zea mays*, respectively.

Subcellular Localization of FRDg in T. brucei and Other Trypanosomatids—To further confirm that FRDg corresponds to the differentially expressed 120-kDa glycosomal protein, specific antibodies were raised against a C-terminal peptide (23 amino acids) deduced from the *FRDg* gene. Western blot analysis on total extracts and glycosomal fractions of *T. brucei* procyclic and bloodstream forms confirmed that the 120-kDa protein is glycosomal and only expressed in the procyclic cells (Fig. 1*B*). In addition, the glycosomal localization was confirmed by an immunofluorescence analysis (Fig. 3). The "glycosome-like" punctuate pattern generated by the anti-FRDg immune serum colocalizes with the signal observed with a monoclonal antibody specific for the glycosomal PPDK (36).

The anti-FRDg specific antibodies recognize a 120-kDa protein in the procyclic form of the closely related African trypanosome *T. congolense* as well as in *C. fasciculata* and *L. amazonensis* (promastigote form) (Fig. 4). This indicates that FRDg is conserved in trypanosomatids. The absence of a signal with the *T. cruzi* epimastigote form could be the result of non-

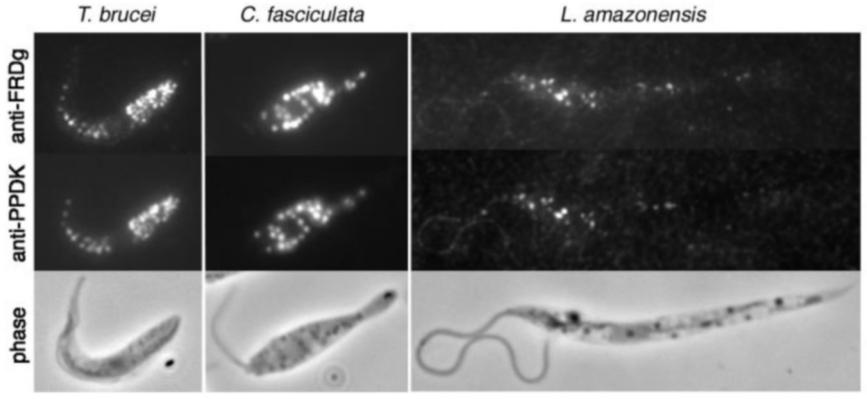

FIG. 3. **Subcellular colocalization of FRDg and PPDK by immunofluorescence analysis.** *T. brucei* procyclic (EATRO1125), *Crithidia fasciculata* (clone HS6) and *Leishmania amazonensis* promastigote (MHOM/BR/87/BA125) cells were stained with anti-FRDg (*top panels*) and anti-PPDK specific antibody (*center panels*). Phase contrast images of the same cells are shown in the *bottom panels*. *Bar*, 5 μm.

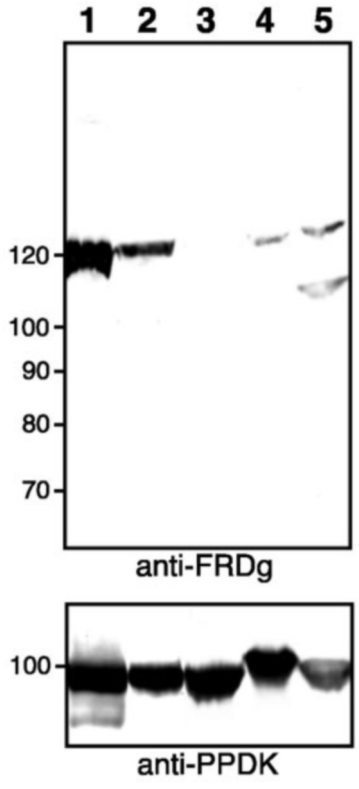

FIG. 4. **Detection of FRDg in different trypanosomatids by Western blot analysis.** Lysates of 2×10^7 cells from the procyclic form of *T. brucei* EATRO1125 (*lane 1*), the procyclic form of *T. congolense* IL3000 clone 49 (*lane 2*), the epimastigote form of *T. cruzi* C. L. (*lane 3*), the *C. fasciculata* clone HS6 (*lane 4*), and the promastigote form of *L. amazonensis* MHOM/BR/87/BA125 (*lane 5*) were analyzed with anti-FRDg (*top panel*) and anti-PPDK (*bottom panel*) antibodies. The position of the molecular mass markers (in kDa) is indicated in the *left margin*.

conservation of the 23-amino acid peptide used to raise antibodies (Fig. 4). Immune sera raised against the central domain of FRDg recognized a 120-kDa protein in *T. cruzi* and all the other trypanosomatids tested, indicating that the epimastigote form of *T. cruzi* expresses FRDg.[2] As observed for *T. brucei*, an immunofluorescence analysis also shows a glycosomal colocalization of FRDg and PPDK in *C. fasciculata* and *L. amazonensis* (Fig. 3).

Characterization of a Glycosomal NADH-dependent Fumarate Reductase Activity—Because of the observed FRDg subcellular localization, procyclic form glycosomes purified by differential centrifugation and isopycnic centrifugation on sucrose gradients as described previously (29) were tested for fumarate reductase activity. The purity of the glycosome preparations was confirmed by the absence of cytosolic (PGK) or mitochondrial (isocitrate dehydrogenase and citrate synthase) activities (data not shown). In contrast, glycosomal enzymes such as PPDK and glycerol-3-phosphate dehydrogenase (GPDH) are 13–15-fold enriched in the glycosomal fractions (Fig. 5) as observed previously (51). NADH-dependent FRD activity was detected in the glycosomes of the procyclic form (142 ± 30 milliunits·mg^{-1} of glycosomal protein). Interestingly, glycosomes also contain a NADH-dependent cytochrome *c* reductase activity (65 ± 21 milliunits·mg^{-1} of glycosomal protein) (Fig. 5). Mracek *et al.* (11) observed previously that a NADH-dependent cytochrome *c* reductase activity, which is not related to the typical mitochondrial enzyme, copurified with the NADH-FRD activity in *T. brucei* and *T. cruzi*. These two NADH-dependent reductase activities are not detected in glycosome preparations of the bloodstream form (data not shown). The low purification factor of these NADH-dependent reductase activities as compared with PPDK or GPDH (2 and 2.5 *versus* 13 and 15) suggests that these activities are unstable and are partially lost during glycosome purification and/or are present in other subcellular compartment(s).

To show the presence of the enzymatic activities inside the organelles, we measured the activities before (α) and after (β) lysis of the glycosomal membrane by sonication. The latency is defined as the percentage of the activity not observable in intact glycosomes ($\beta - \alpha$) with respect to the total activity present in the lysed organelle (β), *i.e.* $((\beta - \alpha)/\beta) \times 100$. For GPDH, a *bona fide* glycosomal protein (38, 52), the latency is 30%. The latency for the NADH-FRD and cytochrome *c* reductase activities are 65 and 60%, respectively, suggesting that both NADH-dependent reductase activities are located inside the glycosome.

The NADH-FRD activity in the *T. brucei* procyclic cells has previously been characterized as a soluble activity that, at low salt concentration, is largely associated with membrane fractions, because ~60% of the NADH-FRD activity was released from these fractions at high ionic strength (150 mM KCl) as opposed to 5% in the absence of KCl (11). In the parasite, most of the NADH-FRD activity is probably soluble as a result of a high intracellular ionic concentration (11). We performed an equivalent experiment on sonicated glycosome preparations of the *T. brucei* procyclic form. Approximately 10, 65, and 80% of the glycosomal NADH-FRD activity is soluble in 0, 100, and 300 mM KCl, respectively, indicating that this glycosomal activity is soluble at high ionic strength.

[2] S. Besteiro, N. Biteau, V. Coustou, T. Baltz, and F. Bringaud, unpublished data.

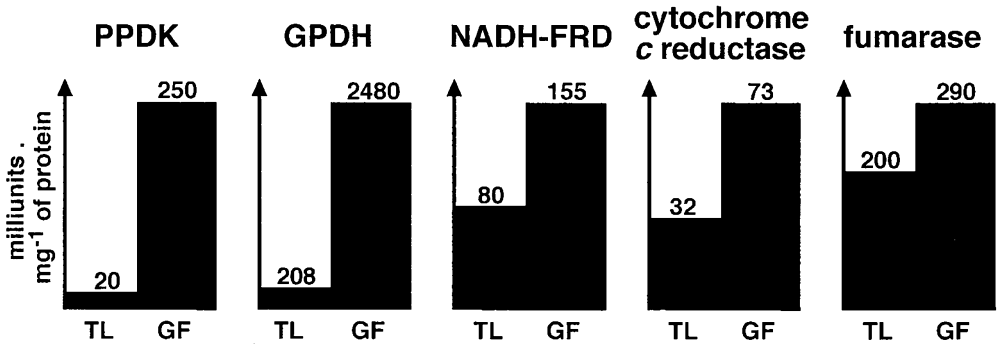

FIG. 5. **Enzymatic activities of purified glycosomes from wild type *T. brucei* procyclic cells (EATRO1125).** The assayed enzymatic activities indicated above each graph were determined in total cell extracts (*TL*) and in glycosomal fractions (*GF*). This figure illustrates one representative experiment from a set of three. The value above each column represents enzymatic activity.

The substrate of FRDg (fumarate) could result from a fumarase activity using L-malate produced in the glycosomes of the procyclic form. Indeed, we detected a fumarase activity (235 ± 55 milliunits·mg^{-1} of glycosomal protein) in the glycosomal fractions of the procyclic form (Fig. 5) but not the bloodstream form. The latency for the fumarase activity determined on glycosomal fractions is 25%, which is consistent with an intraglycosomal localization.

The FRDg Protein Contains NADH-FRD and Cytochrome c Reductase Activities—The results cited above demonstrate that the glycosomes of the *T. brucei* procyclic form contain a FRD-like protein (FRDg) and a NADH-FRD activity. To establish that the FRDg is indeed responsible for this glycosomal NADH-FRD activity, we made a first attempt by expressing the *FRDg* gene in *Escherichia coli* with the pET system (Novagen) and in *Pichia pastoris* with a *Pichia* expression kit (Invitrogen). Unfortunately, both heterologous expression systems failed to produce soluble recombinant proteins for functional assays (data not shown). Therefore, we subsequently used RNAi as an alternative approach. RNAi is a double-stranded RNA (dsRNA)-mediated process occurring in several organisms (17) including *T. brucei* (16), which leads to the specific degradation of the targeted mRNA. To inhibit FRDg expression by RNAi in the procyclic form of *T. brucei*, the pLew79 vector (35) was used to express dsRNA molecules containing linked sense and antisense copies of the targeted *FRDg* sequence under the control of a tetracycline-inducible promoter. The recombinant vector (pLew-FRDg-SAS) was inserted into the rDNA spacer of the EATRO1125.T7T cell line expressing the tetracycline repressor (19, 35). A resistant cell line, EATRO1125.T7T-FRDg.SAS (called ΔFRDg1), was selected without tetracycline to silence the inducible promoter, and tetracycline was added to express the sense/antisense cassette. The effect of dsRNA on FRDg expression was followed by immunofluorescence and Western blot analyses using the PPDK monoclonal antibody as positive control (*inset* of Fig. 6*A*). In the absence of tetracycline the level of FRDg is unaffected, whereas the addition of tetracycline induces the complete disappearance of FRDg. In addition, the pLew-FRDg-SAS expressed in the wild type EATRO1125 strain (EATRO1125-FRDg.SAS cell line, called ΔFRDg2) leads to a constitutive molecular ablation of FRDg. Interestingly, glycosomes isolated from ΔFRDg2 and tetracycline-induced ΔFRDg1 cells contain no detectable NADH-FRD and cytochrome *c* reductase activities, whereas the level of GPDH activity is unaffected (2114 ± 220 and 2036 ± 257 milliunits·mg^{-1} glycosomal protein, respectively). In the glycosomal fraction of the wild type EATRO1125 strain, the NADH-FRD, cytochrome *c* reductase and GPDH activities are 142 ± 30, 65 ± 21, and 2134 ± 357 milliunits·mg^{-1} glycosomal protein, respectively. This clearly shows that both the glycosomal NADH-FRD and cytochrome *c* reductase activities should be attributed to the protein encoded by the *FRDg* gene.

Molecular Ablation of FRDg Affects the Rate of Glucose Consumption—To determine whether the inhibition of FRDg expression affects cell growth, we measured the doubling time of cell lines inhibited or not inhibited for FRDg expression. No difference was observed between wild type and mutant cell lines with a doubling time ranging between 8 and 9 h (Fig. 6*A*). However, both mutant cell lines, wherein a complete disappearance of FRDg was observed, present a reduced ability to acidify the culture medium. Indeed, at the end of the log growth phase, ΔpH (pH at day 3.5 minus pH at day 0) is ~2.3 times lower for the mutants as compared with cell lines expressing FRDg (0.22 and 0.28 *versus* 0.6 and 0.66) (Fig. 6*B*). Because the acidic end products of aerobic glucose metabolism may be responsible for the ΔpH variations, we determined the glucose consumption rate of the same cell lines (Fig. 6*C*). The ΔFRDg2 and tetracycline-induced ΔFRDg1 cell lines consume ~2 times less D-glucose as compared with the EATRO1125 and uninduced ΔFRDg1 cell lines grown under the same conditions (0.62 ± 0.08 and 0.67 ± 0.05 *versus* 1.3 ± 0.05 and 1.22 ± 0.07 μmol·h^{-1}·mg^{-1} of protein). This suggests that the reduction of the growth medium acidification is a direct consequence of the reduced rate of D-glucose consumption observed for the FRDg mutant cell lines.

FRDg Is the Main Source of Succinate Production—We used carbon-13 (^{13}C) NMR spectroscopy for monitoring the metabolic end products secreted by the procyclic cells inactivated or not inactivated for *FRDg* gene expression. These experiments were conducted in the presence of D-[1-^{13}C]glucose as the only carbon source (without L-proline, which is the primary carbon source used by this life cycle stage of the parasite). The parasites were incubated in PBS/$NaHCO_3$ medium containing 110 μmol of D-[1-^{13}C]glucose until 30 μmol of D-glucose was consumed by each cell line. The incubation medium was then analyzed by NMR spectroscopy. To determine the ^{13}C amount in each secreted end product, the analysis was performed on fully relaxed spectra. The wild type EATRO1125 procyclic form mainly secretes succinate, acetate, and lactate. The ^{13}C enrichment of the acetate C2, lactate C3, and succinate at either the C2 or the C3 position are 30.6 ± 0.9, 31.3 ± 5.3, and 22.5 ± 0.6%, respectively. These observed values, significantly lower than the 50% that would be expected from using 100% D-[1-^{13}C]glucose as the sole carbon source, indicate that isotopic dilution occurred through the pathway of glucose catabolism. These low enrichment values cannot be explained by invoking endogenous carbon sources, because African trypanosomes do not contain any kind of carbon storage (6). However, a pentose-phosphate pathway has been described in *T. brucei* (53, 54), and up to 40% of the D-glucose can be utilized by this pathway

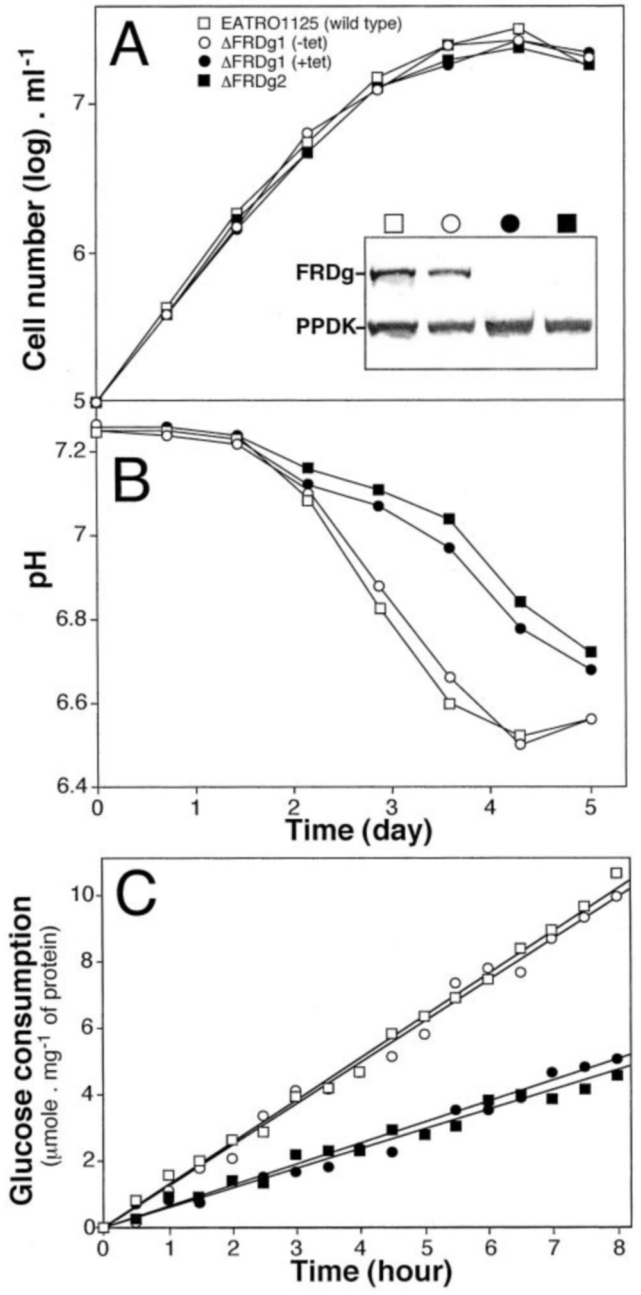

FIG. 6. **Comparative phenotype analysis of FRDg mutant and wild type procyclic cell lines.** Procyclic EATRO1125 cell lines expressing FRDg (□ and ○) or lacking FRDg expression by RNAi (■ and ●) were incubated at 10^5 cells·ml^{-1} in SDM79 medium for 5 days until reaching the stationary phase. For the induced ΔFRDg1 cell line (●), the analyses were performed 10 days after RNAi induction by tetracycline addition. Aliquots were periodically taken to determine cell number and pH to establish the growth curve (*panel A*) and the acidification of the growth medium (*panel B*), respectively. The cell lines analyzed are indicated in *panel A*, and the *inset* in *panel A* represents a Western blot analysis of total protein extracts from the corresponding cell lines using FRDg- and PPDK-specific antibodies. *Panel C* represents the rate of D-glucose consumption (quantity of D-glucose consumed per mg of protein as a function of time) by the same cell lines incubated for 8 h at 10^8 cells·ml^{-1} in SDM79 medium.

in the closely related trypanosomatids *T. cruzi* and *Leishmania* sp. (55, 56). The activity of the pentose-phosphate pathway is likely to be responsible for the observed isotopic dilution, because the enriched C1 glucose will be lost in this pathway due to the decarboxylation reaction of glucose at the C1 position. Then, the non-oxidative branch of the pentose-phosphate pathway produces ^{13}C non-enriched glyceraldehyde 3-phosphate and fructose 6-phosphate, which may be further metabolized by glycolysis. We propose, therefore, that the exchange reaction between the pentose-phosphate pathway and glycolysis accounts for the observed isotopic dilution. Taking into account the calculated percentage of ^{13}C enrichment, ~1401 ± 94, 389 ± 22, and 198 ± 21 mmol of succinate, acetate, and lactate are secreted per mole of D-glucose consumed with low amounts of L-malate and fumarate (23 ± 2.4 and 13 ± 0.8 mmol·mol^{-1} of D-glucose consumed, respectively) (Fig. 7*A*). The same results were obtained with the uninduced ΔFRDg1 cells (data not shown). A similar NMR analysis performed on the FRDg depleted cell line ΔFRDg2 shows that lactate is not secreted and that succinate and acetate productions are reduced by a factor of 2.3 and 1.5, respectively (Fig. 7, *B* and *C*). Interestingly, L-malate and fumarate are abundantly secreted as compared with the wild type cells; their secretion is 20- and 42-fold increased, respectively (Fig. 7, *B* and *C*). Similar results were obtained with the tetracycline-induced ΔFRDg1 cells (data not shown). These data thus show that the elimination of FRDg leads to a concurrent reciprocal change in the secretion of the product (succinate) and substrate (fumarate) of the NADH-FRD reaction, namely a 2.3-fold reduction of the former and a 20-fold increase of the latter. This indicates that FRDg, located within the glycosomes of the *T. brucei* procyclic form, is responsible for the formation of succinate, which is secreted as an end product of glucose metabolism.

The Secreted Succinate Cannot Be Produced in the Tricarboxylic Acid Cycle—The current model of carbohydrate metabolism in the *T. brucei* procyclic form proposes that the secreted succinate is produced in the mitochondrion by a conventional tricarboxylic acid cycle (6). To produce a large amount of succinate, as observed in our experimental conditions, the tricarboxylic acid cycle would have to be fed by dicarboxylic acids (oxaloacetate, L-malate, or fumarate) in addition to acetyl-CoA (see Fig. 8). Because of the absence of any kind of carbon storage in trypanosomes, these molecules are produced from D-[1-^{13}C]glucose. Thus, in the presence of D-[1-^{13}C]glucose as the sole carbon source, the position of ^{13}C enrichment in the succinate molecules depends on the dicarboxylic acid used to feed the tricarboxylic acid cycle. If oxaloacetate, which is produced in the glycosomes or possibly in the mitochondrion from cytosolic phosphoenolpyruvate (PEP), was the source, succinate should be ^{13}C-enriched at both the C2 and C4 positions (Fig. 8*A*). If the tricarboxylic acid cycle were fed by L-malate or fumarate, which are produced in the glycosomes, the situation would be slightly different. Because of the symmetrical structure of these molecules and the reversibility of the reaction catalyzed by fumarase, the same amount of L-malate and fumarate would be labeled at positions C2 and C3 (Fig. 8). This would then lead to the production of the same amount of succinate molecules ^{13}C-enriched at positions C2 and C4 or C2 and C3 (Fig. 8*B*). To test the model proposed by Fairlamb and Opperdoes (6), we determined the relative quantity of succinate molecules ^{13}C-enriched at a single (C2 or C3) or at two (C2 and C3) carbon positions present in the supernatant of wild type and mutant procyclic cell lines incubated with D-[1-^{13}C]glucose as the sole carbon source (Fig. 7, *A* and *B*, *inset*). Because succinate has a symmetrical structure, those molecules that are ^{13}C-enriched at a single position (C2 or C3) are indistinguishable and correspond to a single resonance at 34.88 ppm, whereas those that are ^{13}C-enriched at both C2 and C3 positions resonate as a doublet (36.16 and 33.65 ppm). The area of the satellite peaks indicates that 1.05% (wild type cells) and 1.1% (ΔFRDg2 cell line) of all ^{13}C-enriched succinate molecules (Fig. 7, *A* and *B*, *inset*) were enriched at both the C2 and C3 carbon positions. These values correspond to the natural ^{13}C-

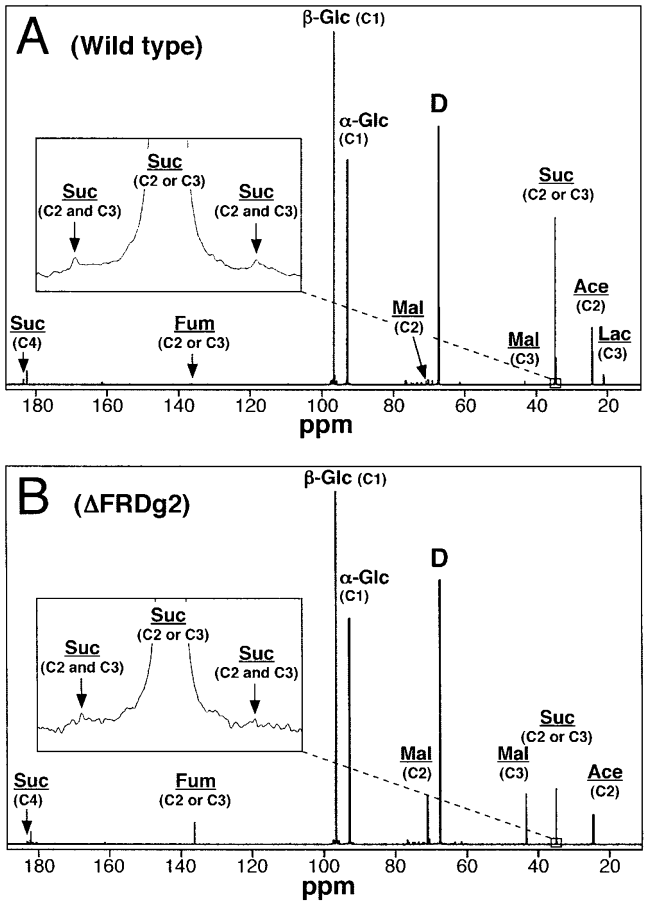

C

	Suc	Ace	Lac	Mal	Fum
Wild type	1401 ±94	389 ±22	198 ±21	23 ±2.4	13 ±0.8
ΔFRDg2	602 ±30	260 ±44	ND	966 ±85	261 ±15
ratio	0.43	0.67	ND	42	20

FIG. 7. **Carbon-13 NMR spectra of metabolic end products secreted by procyclic cell lines incubated with D-[1-^{13}C]glucose.** The incubation medium (PBS/$NaHCO_3$ supplemented with 11 mM D-[1-^{13}C]glucose) containing wild type *T. brucei* procyclic cells (*A*) or the FRDg depleted cell line ΔFRDg2 (*B*) was analyzed by NMR after the addition of 50 μl of dioxane. Each spectrum illustrates one representative experiment from a set of three. The resonances were assigned as follows: *Ace*, acetate; *D*, dioxane; *Fum*, fumarate; *Glc*, D-glucose; *Lac*, lactate; *Mal*, L-malate; and *Suc*, succinate. Underlined resonances correspond to secreted end products. The position of the enriched ^{13}C in each detected molecule is indicated in parentheses. For succinate and fumarate, C2 and C3 resonances are undistinguishable and were labeled *C2* or *C3*. The *insets* (*panels A* and *B*) display the succinate resonance using a scaling factor of ~100 to show the doublet corresponding to succinate molecules ^{13}C-enriched at both the C2 and C3 positions (*C2* and *C3*). A quantitative analysis of these NMR spectra is presented in *panel C*. The values represent mmol of secreted end products per mole of D-glucose consumed (*ND*, not detectable). The last lane shows the ratio between ΔFRDg2 and the wild type cell lines for each secreted end product.

enrichment value (1.1%). The theoretical level of ^{13}C-labeling at both the C2 and C3 position would be in the range of 15%, which corresponds to half of the percentage of ^{13}C-enrichment of the secreted end products. This indicates that succinate cannot be produced by a conventional tricarboxylic acid cycle fed with fumarate or L-malate in addition to acetyl-CoA. Similarly, the area of the peaks corresponding to succinate molecules ^{13}C-enriched at the C4 position (183.2 ppm) is ~1% of the total peak area of the succinate molecules (Fig. 7, *A* and *B*) and corresponds to the natural ^{13}C-enrichment value (1.1%). The theoretical percentage of ^{13}C-labeling at the C4 position of succinate produced by a conventional tricarboxylic acid cycle fed by oxaloacetate would be significantly higher (in the range of 30%, which corresponds to the percentage of ^{13}C-enrichment of the secreted end products). Thus, it is evident from these data that the large majority of the succinate molecules secreted by the procyclic cells is not produced by the tricarboxylic acid cycle.

The T. brucei Procyclic Form Contains a Cytosolic Pyruvate Kinase Activity—In 1986, Fairlamb and Opperdoes (6) proposed a model for carbohydrate metabolism in the *T. brucei* procyclic form (see Fig. 10) that predicts that all PEP produced in the cytosol is further metabolized in the glycosomes due to the apparent absence of a cytosolic pyruvate kinase (PYK) activity. Later, some PYK activity was detected in these parasites (57, 58) but only when its allosteric activator (*i.e.* fructose 2,6-bisphosphate) was added to the assay. Because the activator could not be detected in lysates of the procyclic cells of the strain used by these authors (*T. brucei* 427), no necessity was felt to modify the model by including this enzyme (8). We have now measured the PYK activity (in the absence of its activator) in *T. brucei* strains (EATRO1125 and AnTat1) that are derived from the same *T. brucei* stock and found a different result; the activity in the EATRO1125 procyclic cells is 54 ± 5 milliunits·mg^{-1} protein compared with 1450 ± 120 milliunits·mg^{-1} protein in the AnTat1 bloodstream forms. The relatively low but significant PYK activity detected in the procyclic form (~25 times lower than the bloodstream form) is correlated with the low glucose consumption observed for this adaptative form (~10 times lower as compared with the bloodstream form) (59). It is noteworthy that, under aerobic conditions, the *T. brucei* bloodstream form secretes pyruvate as the only end product of D-glucose metabolism, which is produced by the cytosolic PYK (7).

To determine the subcellular localization of the PYK activity in the procyclic cells, we have carried out a digitonin-titration experiment wherein the different cellular membranes were permeabilized in a controlled way by increasing concentrations of the detergent. Upon increasing the relative concentration of digitonin, the first enzymatic activity to be liberated was PGK, a cytosolic marker, the release of which was complete with 0.06 mg of digitonin·mg^{-1} of protein (Fig. 9). Then, the GPDH and phosphoenolpyruvate carboxykinase (PEPCK) activities, which are located in the glycosomes, are totally released with 0.35 and 0.4 mg of digitonin·mg^{-1} of protein, respectively (Fig. 9). As observed for PGK, all of the PYK activity is released with 0.08 mg of digitonin·mg^{-1} of protein, showing that this enzyme is located in the cytosol of *T. brucei* procyclic form as previously observed for the bloodstream form (7). Interestingly, the main PEP-consuming enzymatic activities detected in procyclic cell extracts, *i.e.* the cytosolic PYK and the glycosomal PEPCK, are in the same range (54 ± 5 *versus* 132 ± 10 milliunits·mg^{-1} of protein). Altogether, these data suggest that, in the growth condition we currently use, a significant amount of PEP is metabolized by PYK in the cytosol of the procyclic form.

DISCUSSION

In the glycosomes of the *T. brucei* procyclic form we have characterized a new 120-kDa enzyme called FRDg, which contains three distinct domains that are significantly similar to ApbE enzymes (thiamine biosynthesis), fumarate reductases, and cytochrome b_5 reductases/nitrate reductases (biosynthesis of unsaturated fatty acids/nitrate metabolism), respectively.

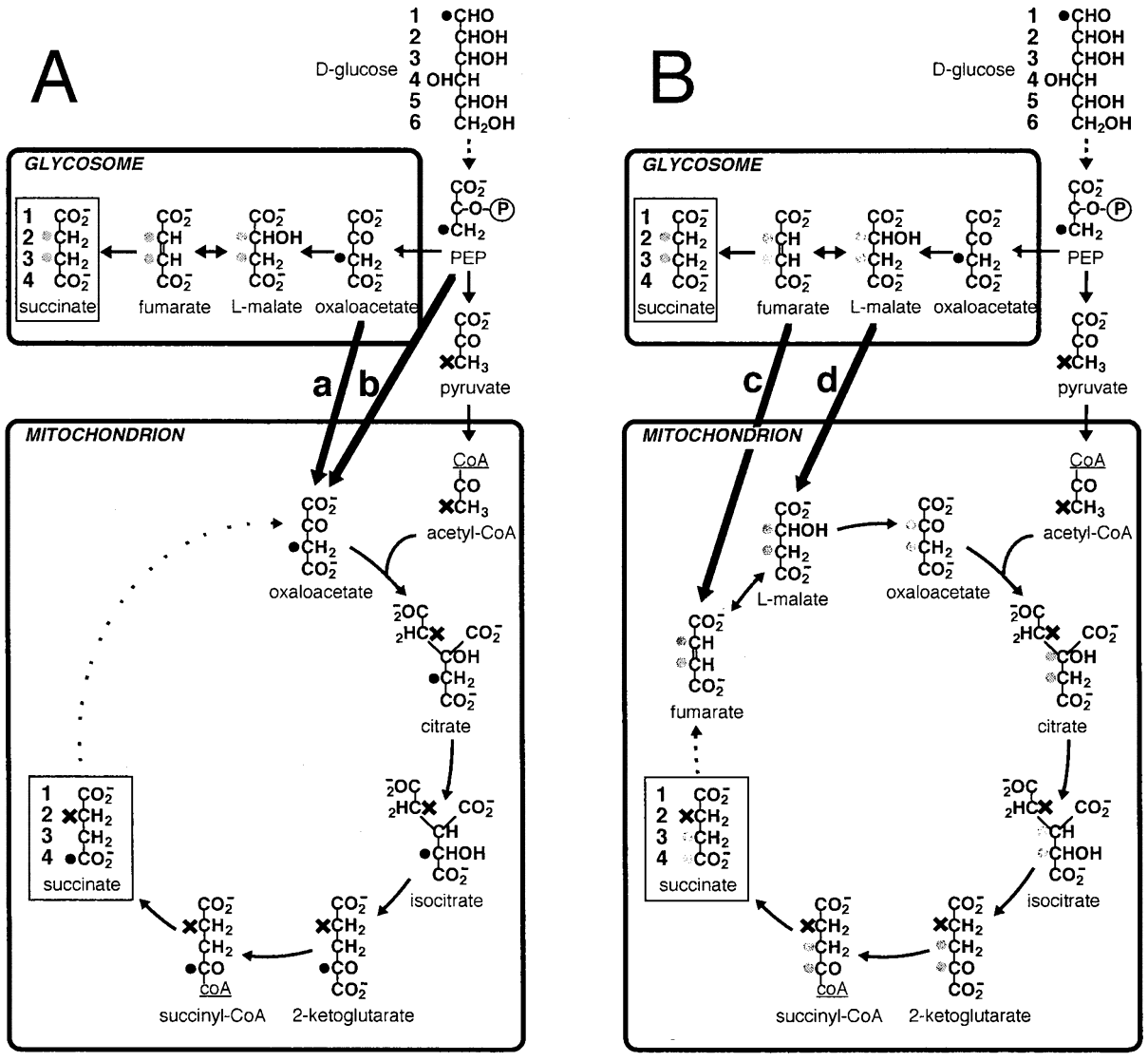

FIG. 8. **Hypothetical pathways for ^{13}C-enriched succinate production in the mitochondrion of the *T. brucei* procyclic form incubated with D-[1-^{13}C]glucose as the sole carbon source.** This figure shows the position of ^{13}C in succinate produced from the tricarboxylic acid cycle fed, in addition to acetyl-CoA, with oxaloacetate (*panel A*) or fumarate or L-malate (*panel B*). *Crosses* and *black* or *gray dots* indicate the ^{13}C. In *panel A*, the tricarboxylic acid cycle is fed with oxaloacetate produced in the glycosomes (*a*) or in the mitochondrion from PEP (*b*), whereas in *panel B* the cycle is fed with fumarate (*c*) or L-malate (*d*) produced in the glycosomes. [1-^{13}C]-D-glucose is metabolized through glycolysis into PEP, which is ^{13}C-enriched at position C3 (10). According to the proposed model (Fig. 10*B*), PEP is transformed into pyruvate in the cytosol (which is further metabolized in the mitochondrion) and into oxaloacetate in the glycosomes to produce succinate. In this model, the tricarboxylic acid cycle is fed with acetyl-CoA ^{13}C-enriched at position C2 (*black dot*). Because fumarate has a symmetrical structure and fumarase catalyzes a reversible reaction, the same amounts of the ^{13}C-enriched L-malate, fumarate, and succinate produced in the glycosomes are labeled at positions C2 or C3 (*gray dots*). The production of PEP from D[1-^{13}C]glucose, described in detail previously (10), is indicated by a *dashed arrow*. The secreted end product (succinate) is boxed, and the enzymatic steps of the tricarboxylic acid cycle, which present a low metabolic flux, are grouped and indicated by a *dashed arrow*.

Considering the unusual structure of FRDg, we cannot rule out the possibility that this enzyme may be a multifunctional protein involved in several branches of metabolism. This enzyme contains a NADH-dependent fumarate reductase activity, and the inactivation of FRDg expression by RNA interference shows that at least 60% of the succinate secreted by the procyclic cells in the presence of D-glucose as the sole carbon source is produced in the glycosomes by FRDg.

As observed for peroxisomes, glycosomes form closed compartments presenting limited exchange of metabolites with the cytosol (9). This implies that the energy (ATP/ADP) and redox (NAD^+/NADH) balances need to be maintained, possibly by the absence of net production and consumption of ATP and NADH by the metabolism inside the glycosomes. In 1986, Fairlamb and Opperdoes (6) proposed a model for carbohydrate metabolism in the *T. brucei* procyclic form. This model, presented in Fig. 10*A*, predicts that NADH produced by glyceraldehyde-3-phosphate dehydrogenase in the glycosomes is reoxidized by the glycosomal L-malate dehydrogenase. Indeed, the 1,3-bisphosphoglycerate produced in the glycosomes reaches the cytosol, where it is transformed into PEP before reentering the glycosomes to be converted into L-malate by the organelle's CO_2 fixation pathway (PEPCK and L-malate dehydrogenase) (Fig. 10*A*). The glycosomal energy and redox balances are thus maintained by the CO_2 fixation pathway if all of the PEP reenters the glycosomes. L-malate would subsequently reach the cytosol, where malic enzyme is supposed to convert it into pyruvate. This model was based on two major observations: (i) the absence of detectable cytosolic pyruvate kinase (PYK) activity, which suggested that all PEP produced in the cytosol should re-enter the glycosome to act as a substrate for PEPCK; and (ii) the absence of a glycosomal fumarase activity, which would

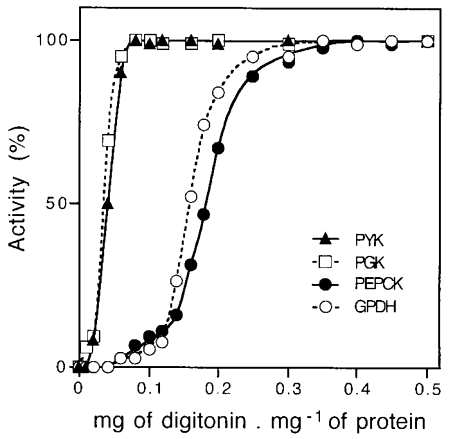

FIG. 9. **Differential release of PYK and various marker enzymes of known subcellular compartments from the intact *T. brucei* procyclic form by titration with digitonin.** The activities of cytosolic (*PGK*) and glycosomal (*GPDH* and *PEPCK*) markers and *PYK* were determined in the supernatant of centrifuged cells after being incubated with 0–0.5 mg of digitonin·mg^{-1} of protein in STE buffer containing 150 mM NaCl. The different concentrations of detergent required for the release of the cellular compartment markers reflect the differences in sensitivity of the plasma membrane and intracellular membranes for digitonin. The activities are indicated as the percentage of the total activity released after sonication of untreated cells.

mean that L-malate is the organelle's end product of glycolysis (6). Since 1986 this model has not been revisited. Here, we showed that the cytosolic PYK activity can be significant. This discrepancy with earlier published data may be due to different growth conditions of the cells. Furthermore, we showed that succinate rather than L-malate is the glycosomal end product of glycolysis.

Consequently, we propose a revised version of the current model concerning the glycosomal and mitochondrial glucose metabolism in the procyclic form of *T. brucei* (Fig. 10*B*). Indeed, these new data suggest that PEP produced in the cytosol is a metabolic branch point, which leads, on the one hand, to acetate and CO_2 production in the mitochondrion *via* PYK and, on the other hand, to the secreted glycosomal end product, *i.e.* succinate. This new model predicts that the flux through the glycosomal CO_2 fixation pathway was overestimated, the consequence of which is the impossibility of the glycosomal L-malate dehydrogenase to maintain the glycosomal redox balance. However, the production of succinate by FRDg is accompanied by NADH oxidation, which implies that, to maintain the redox balance, only half of the PEP produced in the cytosol needs to be transformed into succinate in the glycosome. This suggests that FRDg has a role in the maintenance of the glycosomal redox balance.

However, a corollary of this new model is that the glycosomal ADP/ATP balance could not be maintained because two times more ATP is consumed (hexokinase and phosphofructokinase) than produced (PEP carboxykinase). Our recent finding of a glycosomal PPDK in the procyclic form of *T. brucei* (36) may solve this dilemma concerning the glycosomal energy balance. Interestingly, this enzyme generates two times more high energy bonds per PEP molecule consumed (ATP is produced from AMP) as compared with PEPCK and PYK (ATP is produced from ADP). This property, in conjunction with the glycosomal adenylate kinase activity (6), which exchanges high energy bonds between AMP, ADP and ATP, could make the PPDK enzyme very useful in maintaining the ADP/ATP balance.

Another important issue is the site of succinate production. We showed that more than half (60%) of the secreted succinate is produced in the glycosomes, whereas the remaining 40% may be produced in another compartment. We also showed that succinate cannot be produced by a conventional tricarboxylic acid cycle as opposed to the current model (6) (Fig. 10*A*). However, we detected a non-glycosomal NADH-FRD activity (about one-third of the total cellular NADH-FRD activity) that may be involved in the production of a part (the remaining 40%) of the secreted succinate. Indeed, the FRDg-depleted cell lines lost the glycosomal NADH-FRD activity; however, total cell extracts still contain about one-third of the wild-type NADH-FRD activity (32 ± 5 *versus* 92 ± 12 milliunits·mg^{-1} of protein). The genome of *T. brucei* contains two other genes related to *FRDg*, which may account for this non-glycosomal NADH-FRD activity.[2] Interestingly, Turrens and co-workers (11, 12) characterized a NADH-FRD activity in fractions enriched for mitochondrial markers in *T. cruzi* and *T. brucei*, which may correspond to the non-glycosomal NADH-FRD described here. These authors (11, 60, 61) proposed that succinate produced by this enzyme feeds complex II of the respiratory chain for oxidative phosphorylation. However, we cannot rule out that part of the succinate produced by this NADH-FRD activity is secreted by the parasite. Current work on the other FRD isoforms of *T. brucei* is in progress to address this question.

Among all the trypanosomatids analyzed to date, the bloodstream form of the *T. brucei* group is unique regarding its very simple energy metabolism (9). Indeed, all other trypanosomatids, including the *T. brucei* procyclic form, show a more complex glucose metabolism (8, 10). The following lines of evidence suggest that the proposed revised model may be valid (or in part valid) for all trypanosomatids with the exception of the bloodstream form of the *T. brucei* group. (i) We showed that FRDg homologues are also present in the glycosomes of the *T. cruzi* epimastigote form (data not shown), the *T. congolense* procyclic form, *Crithidia fasciculata*, and the *Leishmania amazonensis* promastigote form. In addition, mining of the *Leishmania major* genome data base identified a full-length gene encoding a FRDg homologue that contains a C-terminal type-1 peroxisome targeting signal (AKI) (www.ebi.ac.uk/blast2/parasites.html). This clearly indicates that the glycosomal NADH-FRD is distributed among trypanosomatids. (ii) The NADH-dependent FRD activity was detected in the *T. congolense* procyclic form (62), the *T. cruzi* epimastigote form (12), *Phytomonas* sp. (40), and the *Leishmania* sp. promastigote form (13). (iii) All trypanosomatids (with the exception of the bloodstream form of the *T. brucei* group, which does not express FRDg) secrete succinate under aerobic conditions (10). (iv) All trypanosomatids analyzed to date contain a cytosolic pyruvate kinase activity, *i.e.* the *T. congolense* procyclic form (62), *T. cruzi* (63), *Phytomonas* sp. (40), *Crithidia luciliae* (64), and the *Leishmania* sp. promastigotes and amastigotes (64, 65). (v) Finally, the glycosomal PPDK is expressed in all trypanosomatids analyzed except the *T. brucei* bloodstream form (36). Consequently, the *T. brucei* procyclic form is a good model for further study of the carbohydrate metabolism of trypanosomatids. However, our knowledge about the metabolism of the intracellular mammalian stage (amastigote form) of the human pathogenic trypanosomatids, *T. cruzi* and *Leishmania* sp., is still rather limited because of the technical difficulties involved in obtaining sufficient numbers of such parasites for biochemical analyses.

The rate of D-glucose consumption is reduced by 50% in the FRDg mutant cell lines, possibly as a direct or indirect consequence of the deficit of the glycosomal NADH-dependent reductase activity. Indeed, in the absence of FRDg, the cells have to adapt the glycosomal metabolism to maintain the NAD^+/NADH balance. However, the enzymes and mechanisms involved in this adaptation are unknown. Interestingly, reduction of the glycolytic flux does not affect the parasite growth

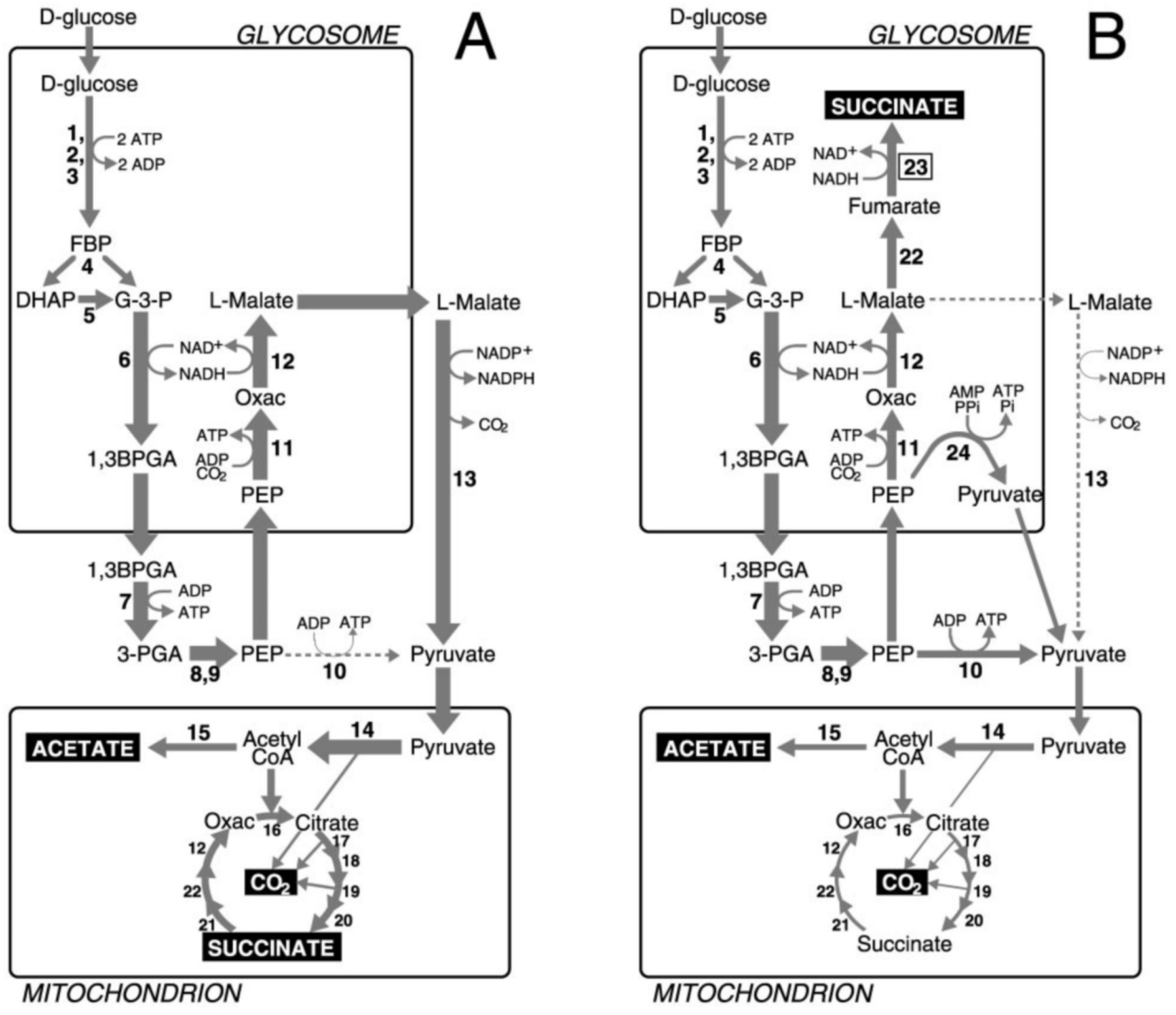

FIG. 10. **Schematic representation of the glycosomal and mitochondrial glucose metabolism in the procyclic form of *T. brucei*.** *Panel A* shows the current model proposed by Fairlamb and Opperdoes (6) and Tielens and Van Hellemond (8), whereas the new proposed model based on the data presented in this paper is shown in *panel B*. The metabolic flux at each enzymatic step is tentatively represented by arrows of different thickness. *Dashed arrows* indicate steps which are supposed to occur at a background level or not at all. Secreted products (succinate, acetate, and CO_2) are in *white characters* on a *black background*. The glycosomal and mitochondrial compartments are indicated, and the number representing FRDg, in *panel B*, is boxed. Abbreviations: *1,3BPGA*, 1,3-bisphosphoglycerate; *DHAP*, dihydroxyacetone phosphate; *FBP*, fructose 1,6-bisphosphate; *G-3-P*, glyceraldehyde 3-phosphate; *Oxac*, oxaloacetate; and *3-PGA*, 3-phosphoglycerate. Enzymes: *1*, hexokinase; *2*, glucose-6-phosphate isomerase; *3*, fructose-6-phosphate 1-kinase; *4*, aldolase; *5*, triose-phosphate isomerase; *6*, glyceraldehyde-3-phosphate dehydrogenase; *7*, phosphoglycerate kinase; *8*, phosphoglycerate mutase; *9*, enolase; *10*, pyruvate kinase; *11*, phospho*enol*pyruvate carboxykinase; *12*, L-malate dehydrogenase; *13*, malic enzyme; *14*, pyruvate dehydrogenase complex; *15*, acetate:succinate CoA transferase; *16*, citrate synthase; *17*, aconitase; *18*, isocitrate dehydrogenase; *19*, 2-ketoglutarate dehydrogenase complex; *20*, succinate CoA synthetase; *21*, succinate dehydrogenase; *22*, fumarase; *23*, NADH-dependent fumarate reductase; *24*, pyruvate phosphate dikinase.

rate, suggesting that this parasite does not use D-glucose as a primary carbon source for its energy supply. Indeed, under the *in vitro* growth conditions used, the *T. brucei* procyclic form uses preferentially amino acids such as L-proline before consuming D-glucose (66). L-proline is an essential component (6 mM) of the SDM-79 medium used to grow the *T. brucei* procyclic form (24).

Most of the FRDs characterized in prokaryotes and eukaryotes to date are associated with membrane multimeric complexes, use quinols as electron donors, participate in electron transfer chains, and are expressed under anaerobic conditions (1). Only very few organisms are known to express a soluble FRD that is not associated with membrane complexes (67). In *Shewanella* sp. the enzyme is expressed under anaerobiosis, accepts electrons from quinols, and is part of an electron transfer chain (4). In *S. cerevisae*, FRDS1 and FRDS2 are expressed under anaerobiosis and use $FADH_2$/$FMNH_2$ as electron donors (2), and *T. brucei* (probably all trypanosomatids) expresses at least one NADH-dependent FRD under aerobiosis. Interestingly, FRDg is the only NADH-dependent FRD characterized so far.

In 1980, H. Gest (68) developed a theory regarding the evolution of biological energy-transducing systems with a key role for FRD. In primitive anaerobic organisms, lactic fermentation of hexoses (glycolysis) evolved to "succinic fermentation" by replacing a NADH-dependent reductase (lactate dehydrogenase) with a four step pathway containing a CO_2 fixation enzyme (PEPCK or pyruvate carboxylase), fumarase, and two

NADH-dependent reductases (L-malate dehydrogenase and a soluble NADH-FRD). This important evolutionary step offered the advantage of requiring 50% less pyruvate (or PEP) to maintain the NAD^+/NADH balance and, consequently, sparing this tricarbon compound for biosynthetic processes. Interestingly, the glycosomal metabolism in the procyclic form of *T. brucei* (and probably all trypanosomatids except the bloodstream form of the *T. brucei* group) resembles the succinic fermentation in primitive anaerobic organisms. As far as we know, FRDg is the only NADH-dependent FRD characterized so far, suggesting that trypanosomatids, which are primitive eukaryotes, are the only known organisms to have conserved the ancestral succinic fermentation.

Acknowledgments—We are extremely grateful to The Institute for Genomic Research and the Wellcome Trust Sanger Institute for all the GSS sequences accessible on the *T. brucei* genome data base (www.ebi.ac.uk/blast2/parasites.html). We particularly thank E. Tetaud and A. Sahin for providing growing cells (*C. fasciculata* and *L. amazonensis*) and D. Baltz for technical help. We also thank P. A. M. Michels, F. R. Opperdoes, and J. Turrens for useful discussions throughout this analysis and P. A. M. Michels and D. R. Robinson for critical reading of the manuscript.

REFERENCES

1. Van Hellemond, J. J., and Tielens, A. G. (1994) *Biochem. J.* **304,** 321–331
2. Muratsubaki, H., Enomoto, K., Ichijoh, Y., Tezuka, T., and Katsume, T. (1994) *Prep. Biochem.* **24,** 289–296
3. Tielens, A. G., and Van Hellemond, J. J. (1998) *Biochim. Biophys. Acta* **1365,** 71–78
4. Pealing, S. L., Black, A. C., Manson, F. D., Ward, F. B., Chapman, S. K., and Reid, G. A. (1992) *Biochemistry* **31,** 12132–12140
5. Arikawa, Y., Enomoto, K., Muratsubaki, H., and Okazaki, M. (1998) *FEMS Microbiol. Lett.* **165,** 111–116
6. Fairlamb, A. H., and Opperdoes, F. R. (1986) in *Carbohydrate Metabolism in Cultured Cells* (Morgan, M. J., ed), pp. 183–224, Plenum Publishing Corp., New York
7. Opperdoes, F. R. (1987) *Annu. Rev. Microbiol.* **41,** 127–151
8. Tielens, A. G. M., and Van Hellemond, J. J. (1998) *Parasitol. Today* **14,** 265–271
9. Michels, P. A., Hannaert, V., and Bringaud, F. (2000) *Parasitol. Today* **16,** 482–489
10. Cazzulo, J. J. (1992) *FASEB J.* **6,** 3153–3161
11. Mracek, J., Snyder, S. J., Chavez, U. B., and Turrens, J. F. (1991) *J. Protozool.* **38,** 554–558
12. Boveris, A., Hertig, C. M., and Turrens, J. F. (1986) *Mol. Biochem. Parasitol.* **19,** 163–169
13. Chen, M., Zhai, L., Christensen, S. B., Theander, T. G., and Kharazmi, A. (2001) *Antimicrob. Agents Chemother.* **45,** 2023–2029
14. Turrens, J. (1999) *Parasitol. Today* **15,** 346–348
15. Tielens, A. G., and Van Hellemond, J. J. (1999) *Parasitol. Today* **15,** 347–348
16. Ngo, H., Tschudi, C., Gull, K., and Ullu, E. (1998) *Proc. Natl. Acad. Sci. U. S. A.* **95,** 14687–14692
17. Fire, A. (1999) *Trends Genet.* **15,** 358–363
18. Bastin, P., Ellis, K., Kohl, L., and Gull, K. (2000) *J. Cell Sci.* **113,** 3321–3328
19. Bringaud, F., Robinson, D. R., Barradeau, S., Biteau, N., Baltz, D., and Baltz, T. (2000) *Mol. Biochem. Parasitol.* **111,** 283–297
20. LaCount, D. J., Bruse, S., Hill, K. L., and Donelson, J. E. (2000) *Mol. Biochem. Parasitol.* **111,** 67–76
21. Shi, H., Djikeng, A., Mark, T., Wirtz, E., Tschudi, C., and Ullu, E. (2000) *RNA* (*N. Y.*) **6,** 1069–1076
22. Wang, Z., Morris, J. C., Drew, M. E., and Englund, P. T. (2000) *J. Biol. Chem.* **275,** 40174–40179
23. Lanham, S. M., and Godfrey, D. G. (1970) *Exp. Parasitol.* **28,** 521–534
24. Brun, R., and Schonenberger, M. (1979) *Acta Trop.* **36,** 289–292
25. Van Meirvenne, N., Janssens, P. G., and Magnus, E. (1975) *Ann. Soc. Belg. Med. Trop.* **55,** 1–23
26. Ross, C. A. (1987) *Acta Trop.* **44,** 293–301
27. Taylor, A. E. R., and Baker, J. R. (1978) *In Vitro Methods for Parasite Cultivation*, Academic Press, London
28. Shim, H., and Fairlamb, A. H. (1988) *J. Gen. Microbiol.* **134,** 807–817
29. Opperdoes, F. R., Borst, P., and Spits, H. (1977) *Eur. J. Biochem.* **76,** 21–28
30. Toner, J. J., and Weber, M. M. (1972) *Biochem. Biophys. Res. Commun.* **46,** 652–660
31. Rosenfeld, J., Capdevielle, J., Guillemot, J. C., and Ferrara, P. (1992) *Anal. Biochem.* **203,** 173–179
32. Bringaud, F., Vedrenne, C., Cuvillier, A., Parzy, D., Baltz, D., Tetaud, E., Pays, E., Venegas, J., Merlin, G., and Baltz, T. (1998) *Mol. Biochem. Parasitol.* **94,** 249–264
33. Thompson, J. D., Higgins, D. G., and Gibson, T. J. (1994) *Nucleic Acids Res.* **22,** 4673–4680
34. Page, R. D. (1996) *Comput. Appl. Biosci.* **12,** 357–358
35. Wirtz, E., Leal, S., Ochatt, C., and Cross, G. A. (1999) *Mol. Biochem. Parasitol.* **99,** 89–101
36. Bringaud, F., Baltz, D., and Baltz, T. (1998) *Proc. Natl. Acad. Sci. U. S. A.* **95,** 7963–7968
37. Callens, M., and Opperdoes, F. R. (1992) *Mol. Biochem. Parasitol.* **50,** 235–243
38. Denise, H., Giroud, C., Barrett, M. P., and Baltz, T. (1999) *Eur. J. Biochem.* **259,** 339–346
39. Misset, O., and Opperdoes, F. R. (1984) *Eur. J. Biochem.* **144,** 475–483
40. Sanchez-Moreno, M., Lasztity, D., Coppens, I., and Opperdoes, F. R. (1992) *Mol. Biochem. Parasitol.* **54,** 185–199
41. Adroher, F. J., Osuna, A., and Lupianez, J. A. (1988) *Arch. Biochem. Biophys.* **267,** 252–261
42. Faloona, G. R., and Srere, P. A. (1969) *Biochemistry* **8,** 4497–4503
43. Hunter, F. R. (1960) *Exp. Parasitol.* **9,** 271–280
44. Marche, S., Michels, P. A., and Opperdoes, F. R. (2000) *Mol. Biochem. Parasitol.* **106,** 83–91
45. Harlow, E., and Lane, D. (eds) (1988) *Antibodies: A Laboratory Manual*, Cold Spring Harbor Laboratory, Cold Spring Harbor, NY
46. Sambrook, J., Fritsch, E. F., and Maniatis, T. (eds) (1989) *Molecular Cloning: A Laboratory Manual*, 2nd Ed., Cold Spring Harbor Laboratory, Cold Spring Harbor, NY
47. Wierenga, R. K., Swinkels, B., Michels, P. A., Osinga, K., Misset, O., Van Beeumen, J., Gibson, W. C., Postma, J. P., Borst, P., Opperdoes, F. R., and Hol, W. G. J. (1987) *EMBO J.* **6,** 215–221
48. Sommer, J. M., and Wang, C. C. (1994) *Annu. Rev. Microbiol.* **48,** 105–138
49. Begley, T. P., Downs, D. M., Ealick, S. E., McLafferty, F. W., Van Loon, A. P., Taylor, S., Campobasso, N., Chiu, H. J., Kinsland, C., Reddick, J. J., and Xi, J. (1999) *Arch. Microbiol.* **171,** 293–300
50. Hyde, G. E., Crawford, N. M., and Campbell, W. H. (1991) *J. Biol. Chem.* **266,** 23542–23547
51. Opperdoes, F. R., Baudhuin, P., Coppens, I., De Roe, C., Edwards, S. W., Weijers, P. J., and Misset, O. (1984) *J. Cell Biol.* **98,** 1178–1184
52. Kohl, L., Drmota, T., Thi, C. D., Callens, M., Van Beeumen, J., Opperdoes, F. R., and Michels, P. A. (1996) *Mol. Biochem. Parasitol.* **76(1–2),** 159–173
53. Cronin, C. N., Nolan, D. P., and Voorheis, H. P. (1989) *FEBS Lett.* **244,** 26–30
54. Barrett, M. P. (1997) *Parasitol. Today* **13,** 11–15
55. Bowman, I. B. R., Tobie, E. J., and Von Brandt, T. (1963) *Comp. Biochem. Physiol.* **9,** 105–114
56. Marr, J. J. (1980) in *Biochemistry and Physiology of Protozoa* (Levandowsky, M., and Hunter, S. H., eds) Vol. 3, pp. 313–340, Academic Press, New York
57. Misset, O., Van Beeumen, J., Lambeir, A. M., Van der Meer, R., and Opperdoes, F. R. (1987) *Eur. J. Biochem.* **162,** 501–507
58. Callens, M., Kuntz, D. A., and Opperdoes, F. R. (1991) *Mol. Biochem. Parasitol.* **47,** 19–29
59. Ryley, J. F. (1962) *Biochem. J.* **85,** 211–223
60. Turrens, J. F. (1989) *Biochem. J.* **259,** 363–368
61. Denicola-Seoane, A., Rubbo, H., Prodanov, E., and Turrens, J. F. (1992) *Mol. Biochem. Parasitol.* **54,** 43–50
62. Obungu, V. H., Kiaira, J. K., Olembo, N. K., and Njobu, M. R. (1999) *Indian J. Biochem. Biophys.* **36,** 305–311
63. Cazzulo, J. J., Cazzulo Franke, M. C., and Franke de Cazzulo, B. M. (1989) *FEMS Microbiol. Lett.* **50,** 259–263
64. Van Schaftingen, E., Opperdoes, F. R., and Hers, H. G. (1985) *Eur. J. Biochem.* **153,** 403–406
65. Adje, C. A., Opperdoes, F. R., and Michels, P. A. (1997) *Mol. Biochem. Parasitol.* **90,** 155–168
66. ter Kuile, B. H. (1997) *J. Bacteriol.* **179,** 4699–4705
67. Hederstedt, L. (1999) *Science* **284,** 1941–1942
68. Gest, H. (1980) *FEMS Microbiol. Lett.* **7,** 73–77